Dual-frequency and Multi-polarization Shuttle imaging Radar for Volcano Detection in Kunlun Mountain of Western China

Guo Huadong, Liao Jingjuan, Wang Changlin, Wang Chao
(Institute of Remote Sensing Applications, Chinese Academy of Sciences, Beijing 100101, China)

Thomas G. Farr and Diane L. Evans
(Jet Propulsion Laboratory, California Institute of Technology, Pasadena, California, USA)

Abstract

A group of volcanoes to the northeast of Aksayqin Lake, western Kunlun, China, are identified from dual-band, multi-polarization SIR-C/X-SAR image, and most of them are discovered by the authors with the SAR data. This paper discusses the methods and mechanisms of detecting volcanoes using L, C bands and HH, HV, VV polarization imaging radar, and gives the spatial distributions of volcanoes elevated more than 5300m above the sea level, eruptive phases and analytical results of rock components.

1. Introduction

The characteristics of transmiting microwave pulses from the sideways of synthetic aperture radar (SAR) can accentuate topographical features, while the sensitivity of SAR to the surface roughness enables it to give markedly details about the surface. These advantages of SAR make it very effective to recognize volcanic apparatus. The studies on volcanoes have been conducted successfully using images of shuttle imaging radar and other spaceborne SAR (Gaddis et al., 1989, 1990; Mouginis-Mark, 1995; Rowland et al., 1994). Airborne SAR also plays an important role in the studies on volcanoes (Lewis and Guo, 1991; Liu et al., 1992). The discovery of volcanoes on Venus was only made by using SAR techniques (Head et al., 1992). At present, the successful flown of SIR-C/X-SAR and its simultaneously imaging characteristics of multi-band, multi-polarization of SIR-C/X-SAR provide new techniques for studying Volcanoes.

On 17 April 1994, the shuttle "Endeavor" equipped with SIR-C/X-SAR system was flown over China and for the first time obtained multi-band, multi-polarization SAR data for Kunlun area (Farr, 1993). During image processing and analysis for SAR data, a group of volcanoes were identified. The authors, thereafter, conducted field work in the study area and proved further for the existence of these volcanoes.

2. Geology of the Study Area

The study area is situated in the northwest of Qinghai-Tibet plateau of China, northeast of Aksayqin Lake in Kunlun Mountain, anti about 60 km to the east of Xinjiang-Tibet road (Fig. 1). This is a high relief anti arid to semi-arid area where elevation is about 5000 - 6000 m above the sea level. The climate is cold. Modern glaciers are well developed, and moraine deposits of palaco-glaciers are widely distributed. Vegetation is rare. Rock outcrops are very well. Alluvial fans flanking the mountain front are widely developed. Tectonically, the study area lies in the eastern part on the southern side of Kangxiwa fault (also called Karakashi Valley fault). Tarim basin is to the north and Tibetan-Indian plate to the south. Lithologies in the study area ranged from old to young ages are mainly composed of Lower Palaeozoic meso-metamorphic complex, Palaeozoic marine sedimentary rocks, Mesozoic and Cenozoic sedimentary rocks of" continental- oceanic phase, together with intermediate to acidic igneous rocks of Caledonian, Variscan, Indosinian-Yanshan epoches.

Fig. 1 Location map of the study area.

Geological study in this area is at a rather poor level due to lacking, of oxygen in the high relief Mountain, and poor working environment. The studies of volcanoes in this area are few. According to the literatures as far as we know, the earliest published paper reporting the existence of volcanoes in the area was from Zhang et al. (1987), which simply introduced that there is a shield volcanic crater elevated several hundred meters above the surface and gave an airphoto to illustrate the shape of the crater. In the Qinghai-Tibet Plateau Al(as published by the Geography Institute, Chinese Academy of Sciences (1 990) inferred the existence of volcanoes. In the papers published by Deng (1 989, 1 991, 1993, 1995) and Arnaud et al. (1992) about Cenozoic volcanoes of Qinghai-Tibet plateau only reported some rock geochemical data. The Geological Memoirs of Regional Geology of Xinjiang Uygur Autonomous Region published by the Bureau of Geology and Mineral Resources of Xinjiang (1993) said there are four craters in the region, which is up to now the best description for the volcanoes in the area.

3. Analysis of **Multi-frequency and Multi-polarization SIR-C Data**

3.1 Data Acquisition

SIR-C/X-SAR was operated in mode. 11 for the study area, i .e., imaging under the combinations of L-HH, L-HV, C-HH and C-VV. The imaging parameters are given in 'Table 1. In the meanwhile, the ERS-1 SAR data with C band and VV polarization mode also have been acquire.d.

Table 1. SIR-C/X-SAR Imaging Technical Parameters for the Study Area

3.2 SIR-C data for the discovery of volcanoes

After image processing for the obtained SIR-C data with L, C bands and HH, HV, polarization, false colour images were produced by multi-band, multi-polarization combinations (1 'ig.2), which reflect the appearances of volcanoes. In particularl y, the combination of' 1,-1111, 1 .-1 1V and C-1 IV images can explicitly delineate the outlines of the whole vole.allic area. According to the composite image of multi-band, multi-polarization, identifications can be made for different shapes and types of volcanic craters and calderas, A 'a and pahoehoe lave flows, lava escarpments, and the boundary of lava flows and surrounding strata (1 'ig.3).

Fig.2 False colour composite images of multi-band, mulit-polarization SIR-C data
a) Composite image of 1,-1111 (R), L-HV (G) and C-HV (B)
b) Composite image of 1 .- HH (R), 1 .-HV (G) and C-HH (B)
both can give the whole volcanic appearances, but (a) shows better effect.

1 'ig.3 Geological interpretation map for SIR-C image. No. 5-9 arc calderas discovered in this study. 1) craters and numbers, 2) A 'a lava, 3) pahochoe lava, 4) Triassic strata . 5) Quanternary Sediments

Nine different c.raters and calderas appear in different shapes and tones on the SIR-C image. The No. 1, 2, 3, 4 craters among them, which reflect positive landform, appear very bright and very obvious, and can be discovered easil y in the field, therefore, they were mentioned in the literatures (Zhang et al., 1 987; Bureau of Geology and Mineral Resources of Xinjiang Uygur Autonomous Region, 1993). The No. 1 crater is the largest one in this region with area of 2.14 Km^2 and in oval shield shape, the centre coordinate of which is longitude 80°1 1 ' and latitude 35°30'. The No. 2, 3 craters are less than 1 Km^2 in area and in cone shapes. The No. 4 crater is also in cone shape, but its area is just less than the No. 1 crater (1 .932 Km^2). The No. 5, 6, 7, 8 and 9 arc calderas which arc in circular radiating shape, and do not have large difference in elevation with the surfaces around. As they are surrounded by the huge lava flows and covered by the surface materials, (hey can not be easily distinguished in the field. These calderas are discovered in this study using S1 R-C imagery. Because of the corner reflector effect caused by the radar beams illuminating the cliff by the side-looking radar, they appear in ring shape or half-ring shape on the image. The areas for the original cone craters are less than 1 Km^2, but it increase to 3-4 Km^2 after their collapses. The main components of the crater rocks are amygdaloidal pyroxene andesite.

Two types of lava flows (A 'a lava and pahoehoe lava) have different radar response on the SIR-C colour composite images. A' a lava flows are mainly distributed around craters No. 5, 6, 7, 8, and their brightness are relatively darker than that of craters No. 1, 2, 3 and 4. The surrounding surfaces of calderas mainly consist of angular rocks piled one on the other without any order. The largest one can reach above 1 m. Vesicular and almond-structures are well developed in the rocks. Lithologies for the rocks are mainly amygdaloidal basalt and trachybasalt. The area for A 'a lava flows is 22..636 Km^2, which is derived from digiti~.ii):>, the boundary of this type lava flow from the screen using PCI software and then input into ARC/INFO for the areal calculation.

Pahoehoe lava is mainly distributed on the southern side of craters. It extends in near N-S direction about 23 km in length, and 10 12 Km in width and about 107 m in depth. The statistical area is 59.470 Km^2. It occurs near horizontally in a fan shape, and unconformably overlay Triassic strata. The surface is relatively flat and covered by Quaternary sediments, showing a relative dark tone on the S1 R-C image. Lithologies for the rocks are dorgalite and pyroxene basalt.

The escarpments of lava flows were produced when flowing pahoehoe lava on the surface were affected by topographical features. They are in bright lines and can be recognized easily when facing to the illumination of radar antenna. These escarpments delineate the shape of lava flows very well and therefore can distinguish lava flows from strata clearly on the image.

3.3. 1 Effect of single band, single polarization SAR for detecting volcanoes

Radar image reflects the scattering characteristics of ground materials. The brightness of radar image depends on the variations of the intensity of radar's backscattering. The radar scattering coefficient σ^0 quantitatively represents the intensity of energy of the return pulse, which is determined by two types of factors: one is radar system parameters, i.e. wavelength, polarization and look angle; another is the object parameters including, the surface roughness and complex dielectric constant of the surface materials. Using multi-band, multi polarization SIR-C image can detect volcanic landform in different occurrences, but radar images with different band and different polarization can have different detecting abilities to the products of different volcanism (Fig. 4).

Fig. 4 Single-~Jan(li single polarization SIR-C images. a) L-HH, b) L-HV, c) C-HH, d) C-HV. L-HV SIR-C image give good result than the others in recognizing volcanic lava flows.

Volcanic apparatus is shown much clearly on L band image than that on C band image, which has the same implication for the identification of lava flows and the contact boundary between lava flows and the surrounding strata. L band has a long wavelength and certain penetration ability to dry sands and other surface materials (Sabins, 1986; Blom et al., 1984). Therefore, L band image appears more clearly than C band for the surface covered by thin layer of sand over pahoehoe lava as well as the contact zone between lava and strata. L band image also shows craters and A'a lava more clear than C band image. The measurement of complex dielectric constant (Fig.5) indicates that the complex dielectric constants of volcanic rocks are not related to a large extent to the frequency of' electromagnetic wave. The variation of complex dielectric constant varies mainly from 3+(- I)i to 8+i, indicating the influence of radar return by complex dielectric constant is little. The different volcanic landforms reflected on different bands of radar image are mainly due to the effect of surface roughness .

Fig. 5 Complex dielectric constant for volcanic rocks under different frequency, the upper part represents the real quantity and lower part denotes imaginary quantity.

Fig. 6. Radar response curves of craters and lava flows denoted by averaging DN value. Among the curve, patterns for A' a lava flow and pahochoe flow are resemble each other, while the curves for craters and lava flows arc different from each other.

The nature of the surface objects have influences on polarization. Polarization is produced by the variation of the vector of electronic field through prop agation, reflection, scattering and diffraction. Therefore, strong depolarization often occurs on the rough surface. Although the radar return for lava flows on HV image is not as strong as that on 1111 image (Fig.6), the effect on HV image is, however, better than that on HH image since lava flow is a strong depolarized body. For the like-polali~,cd images, VV polarization is very sensitive than I 1 I 1 polarization to the rough surfaces, therefore, the ERS-1 image of C band, VV polarization (Fig.7) is very clear for lava flows than that shown on ~-l111 image of SIR-C data. However, the illuminat ion direction of ERS-1 is from east to the west, and the incidence angle is relatively small (230), the resultant image contains a 101 of layover and foreshortening, and therefore, has large distortion. A 'a lava flows and calderas arc not easily seen on the ERS-1 image.

Fig. 7 ERS- 1 SAR image with C-band VV polarization. The Cl'atCl's and pahoehoe lavas can be seen, but A' a lavas and calderas cannot be distinguished from the image.

A comparative analysis (Table 2) for radar images of different band and different polarization suggests that 1. band HV polarization reflects most explicitly the topography and landforms of the whole volcanoes as well as the landforms of the surrounding areas. Although 1,-1111 image can also reflect some features revealed by 1,-HV image, it is not as clear as that on I , 1 IV image. The C band images are obviously not as good as 1. band images concerning their effects on reflecting geological information. The boundaries between A 'a lava and pahoehoe lava are not easily identified, so do the calderas. While the ERS-1 C-VV image likely can not reflect the composition of the whole vole.alliv apparatus. The C-HV image can only give us roughly the whole appearance of the volcanoes. Therefore, there are some limitations for single band, single polarization radar images in identifying and detecting volcanoes. The solution is to use multi-band, multi-polarization radar data to compensate the shortcomings of each other so as to achieve the goal of recognizing and detecting volcanoes.

'1'able 2. The response of different bands and different polarization radar to volcanic landforms

4. Results on geological study

The group of volcanoes to the northeast of Aksayqin Lake, western Kunlun Mountain, belongs to continental central eruption. '1 he eruptive centre is located on the DahongJiutan fault. The volcanic apparatus is controlled by NW fault. The SIR-C image shows nine craters of shield shapes, cone shapes and radiating ring-like calderas, together with lava flows distributed from northern high relief to the southern low relief. The volcanic rocks are mostly in dark grey and brick red colors. Vesicular and amygdaloidal structures are well developed Rocks around the craters and to the north of it contain dense and large vesicular openings, while the vesicular openings are getting smaller towards the south and distributed sparsely. According to the analysis based on the profiles across the lava flow suggests that there were at least two phases of eruptions: one is dorgalite pyroxene basalt, and the other is trachybasalt to tracyte in rock compositions. Grits and siltstones were deposited during the gaps of two eruptive periods. The K-Ar isotope dating for the samples collected from lava flows suggests the age of 7.45 to 3.97 Ma, i.e., from Miocene epoch to Pliocene epoch. The ages of samples from the lava flow are getting young from the south to the north, indicating that there are evidence for multiple eruptions, and the closer to the craters, the younger of the eruption is. Although radar data can not give directly the evidence of the ages of the lava flow, the study by Gaddis et al. (1 989) suggests that the brightness variations of radar image can directly provide information about the ages of lava flows, i .e., the most bright lava flows on radar image have younger age and formed at the last stage, while with the increase of' the age, the brightness on the image is getting darker. Therefore, the study of volcanoes from the image accords with the result of isotope dating.

Studies on the petrography and chemical composition analysis for the volcanic samples collected in the field suggest that the crystallization of volcanic rocks is at a low level, and there are minor amount of pyroxene and olivine crystals which have been subjected to iddingsite alteration; matrix are in hyalopilitic texture. Chemically, potassium content is very high, K_2O is commonly higher than 4%o, and $K_2O > Na_2O$. The Rb, Sr, Ba, Nb, 'J's and other minor trace elements and light rare earth elements are enriched, and basically do not show Eu anomaly. The rocks belong to shoshonitic series. The shoshonitic rocks have special distribution pattern in the orogenic evolution of the plate tectonics, and are mainly related to the intracontinental subduction zone (Jackes and White, 1971), The shoshonitic rocks in Kunlun Mountain are associated with the neotectonism of Qinghai-Tibet Plateau since Cenozoic era, The volcanic eruption maybe caused by the rapid ascending magma produced by the subduction of Tarim plate southerly plunging into the crust underneath he Qinghai-Tibet Plateau (Deng, 1989, 1993).

5. Conclusion

A group of volcanoes consist of nine craters were identified from the western Kunlun Mountain of China by analyzing SIR-C data, and five of nine volcanoes arc discovered in this study. Meanwhile, the areas of A'a lava and pahoehoe lava are calculated as 22.636Km^2 ant] 59.470Km^2 respectively from screen digitizing the outlines of two types of lava flows using PCI software and then input into ARC/INFO to get the precise distribution dimensions of the lavas. The volcanoes, elevated from 5300m to 5800m above the sea level, arc one of the highest volcanoes in the world, There were at least two eruptive phases of' the volcanoes. Isotope dating suggests the ages of volcanoes are 7.45 - 3.97 Ma. The volcanic rocks belong to shoshonitic series, The volcanism is related to the intracontinental subduction produced by the! Tarim plate plunging into the crust underneath the Qinghai-Tibet plateau, which rc.presents the neotectonism of Qinghai-Tibet plateau since Cenozoic era. It has an important significance to the study of neotectonism in Qinghai-Tibet plateau.

The volcanic apparatus is discovered by using dual-band, multi-polarization SIR-C data, indicating, that multi-band, multi-polarization imaging radar can reveal much more geological information. As far as single band, single polarization SAR data arc concerned, L-HV has much better detection effect than C-HH, C-HV and C-VV images. The authors, therefore, suggest that above effects arc caused by the depolarization and surface roughness of the lava flows.

Acknowledgments

The authors would like 10 extend their sine.crc thanks to all members of Xinjiang team who participated in the field work to conduct geological study and SIR-C data investigation in Kunlun Mountain. Special thanks are given to Dr. C. Elachi, Dr. G Peltzer, Dr. O. Chadwick of" J]']. and Dr. R J. Ryerson of Lawrence Livemore National Laboratory, University of California, and Dr. D. Clark of University of' Washington for their collaborative works in the field. Mr. Dai Xibo of IRSA is appreciated for his logistic works in the field, and Mr. Li Junfei of IRSA is acknowledged for his help on measuring the complex dielectric constants of rock samples. This research work is also founded by the Commission of Nations] Natural Science Foundation of China, which is therefore deserved special thanks for their support.

References

Arnaud, N. O., Vidal, Ph., Tapponnier, P., Matte, Ph., and Deng, W. (1992), The high-K_2O volcanism of northwestern Tibet: geochemistry and tectonic implications, *Earth and Planetary Science Letters*, 111:351-367.

Blom, R. G., Crippen R. J., and Elachi, C. (1 984), Detection of subsurface feature in Seasat radar images of Means Valley, Majave Desert (California, Geology, Vol. 12, pp. 346-349.

Bureau of Geology and Mineral Resources of Xinjiang Uygur Autonomous Region (1993), Geological memoirs (series 1, number 32): regional geology of Xinjiang Uygur Autonomous Region, Geological Publishing House, Beijing. pp. 376-378.

Deng, W. (1989), Cenozoic volcanic rocks in the northern Ngari district of the Tibet (Xizang) - discussion on the concurrent intracontinental subduction, *Acta Petrological Sinica*, No. 3, pp. I-11.

Deng, W. (1 991), Geology, geochemistry and age of shoshonitic lavas in the central Kunlun orogenic belt, *Scientia Geologica Sinica*, No. 3201-213.

Deng, W. (1 993), Study on trace element and Sr, Nd isotopeic geochemistry of Cenozoic potassic volcanic. rocks in North Tibet, *Acta Petrological Sinica*, Vol. 9, pp. 379-387.

Deng, W. (1995), Cenozoic magmatic activities and lithospheric evolution of the Qinghai-Xizang Plateau, in *Studies on the evolution of the formation of Qinghai-Xizang Plateau, migration of environment and Ecology System*. pp. 288-296.

Farr, T. G., (1993), Climate change and neotectonic history of northwestern China, SIR-C/X-SAR mission overview, JPL Publication 93-29.

Gaddis, L. R., Mouginis-Mark, P., Singer, R., and Kaupp, V. (1 989), Geologic analysis of shuttle imaging radar (SIR-B) data of Kilauea Volcano, Hawaii, *Bulletin of the Geological Society of America.*, 101, 317-374.

Gaddis, L. R., Mouginis-Mark, P., and Hayashi, J. N. (1990), Lava flow surface textures: SIR-B radar image texture, field observations, and terrain measurements, *Photogrammetric Engineering and Remote Sensing*, 56 (2): 211224.

Guo, 11. D. (1991), Radar geology and its progress, in *Radar Image Analysis and Geological Application,* Science Press, Beijing, pp. 1-10.

Head, J. W., Crumpler, L. S., and Aubele, J. C. (1992), Venus volcanism: classification of volcanic features and structures associations, and global distribution from Megellan data, *Journal of Geophysical Research*, Vo]. 97, No. E8, pp. 13153-13157.

Institute of Geography, Chinese Academy of Sciences (1 990), The altas of Qi@lai-Tibet plateau, Science l'less, Beijing.

Jackes, 1'. and White A. J. (1971), Composition of island arc and continental growth, *Earth Planet Science Letters, No.* 12, pp.224 *-2.36.*

Lewis, A. J., Guo, 11, D., (1991), Evaluation of X band multi-polarization radar image for St. Helen volcanoes, in *Radar Image Analysis and Geological Application,* Science Press, Beijing, pp. 99-102..

Liu, 11., Wci, X. 1'., Wang, C., She, Y. (1 992), Ring structure and volcanic system in Datong region using airborne SAR image, in *Experimental Study on Airborne Radar Remote Sensing Applications, Chinese* Science and Technology Pros, Beijing, pp. 112-125.

Mouginis-mark, 1'. J. (1995), Preliminary observations of volcanoes with the SIR-C radar, *IEEE Trans. on Geosci. and Remote Sensing, 33(4): 934-941,*

Rowland, S. K., Smith, G. A., and Mouginis-Mark, P. J. (1994), Preliminary ERS-1 observations of Alaskan and Aleutian volcanoes, *Remote Sensing of Environment*, 48: 358-369.

Sabins, F. F, Jr. (1 986), *Remote sensing principles and interpretation*, Second Edition, W. 11. Freeman and Company, New York.

Zhang, Z. D., Li, G. 1... and Yang, D. I'. (1987), The geological characteristics, formation and development of Kangx i wa fault, *Xinjinag Geology, 5(3): 50-57.*

1 ,ist of Figures

List ofrl'able.s

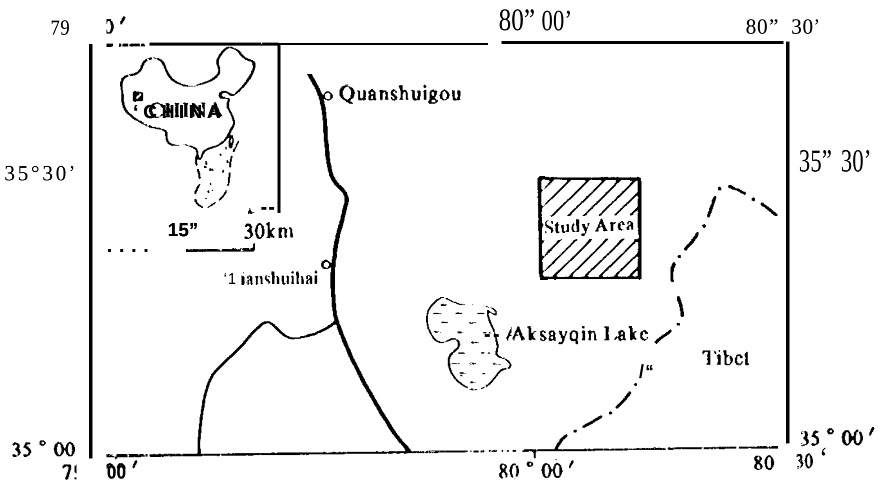

Fig.1 Location map of the study area.

a b

Fig.2 False colour composite images of multi-band, mulit-polarization SIR-C data
a) Composite image of L-HH (R), L-HV (G) and C-HV (B)
b) Composite image of L-HH (R), L-HV (G) and C-HH (B)
both can give the whole volcanic appearances, but (a) shows better effect.

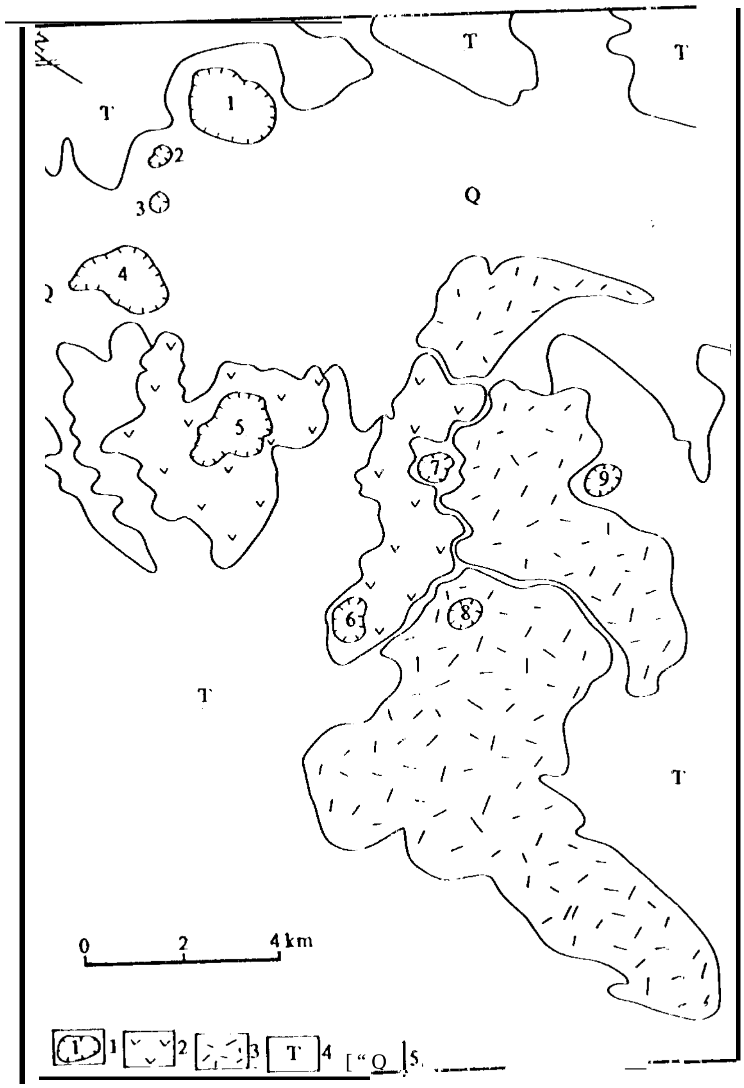

Fig. 3 Geological interpretation map for SIR-C image. No. 5-9 are calderas discovered in this study. 1) craters and numbers, 2) A' a lava, 3) pahoehoe lava, 4) Triassic strata, 5) Quanternary Sediments

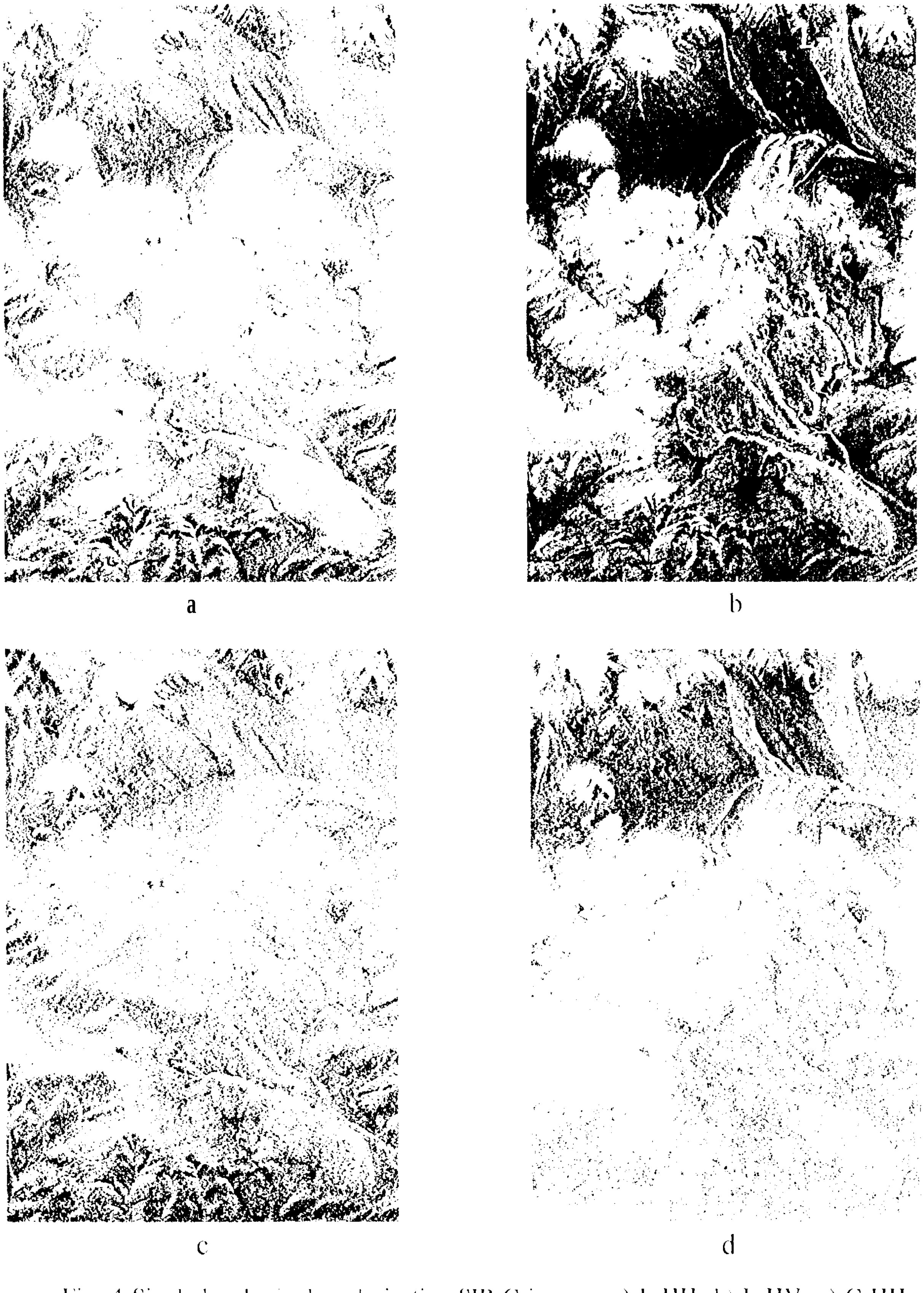

Fig. 4 Single-band, single polarization SIR-C images. a) L-HH, b) L-HV, c) C-HH, d) C-HV. L-HV SIR-C image give good result than the others in recognizing volcanic lava flows.

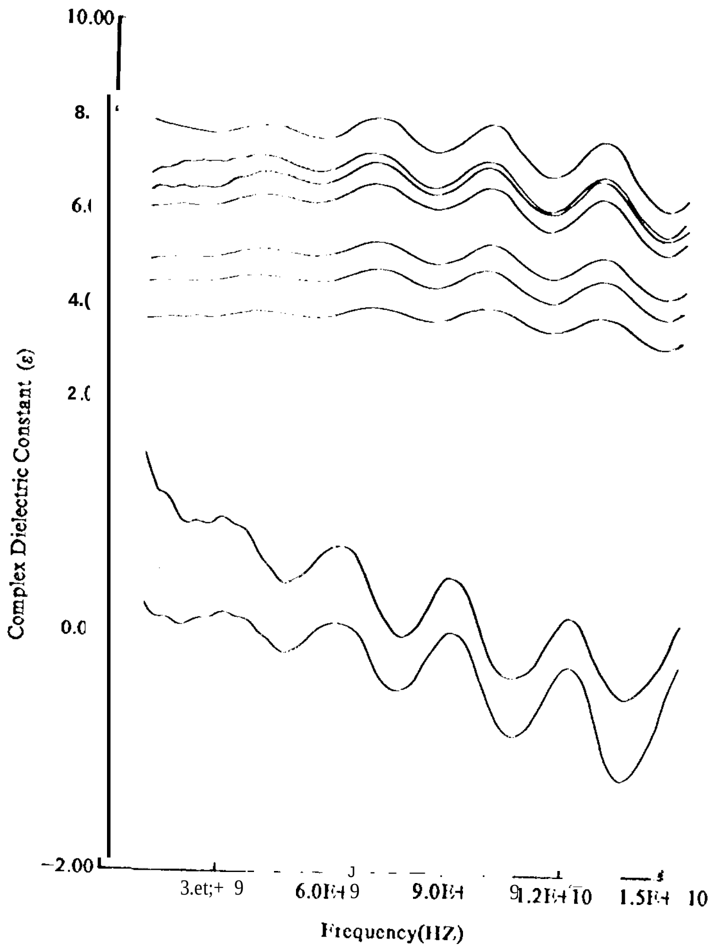

Fig. 5 Complex dielectric constant for volcanic rocks under different frequency, the upper part represents the real quantity and lower part denotes imaginary quantity.

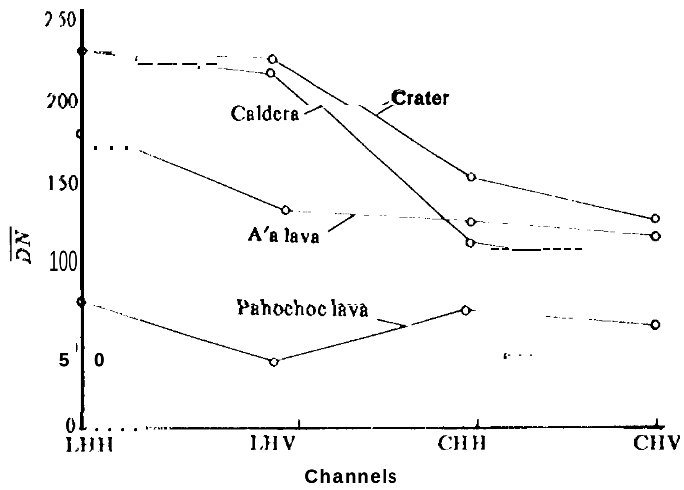

Fig. 6. Radar response curves of craters and lava' flows denoted by averaging DN value. Among the curve, patterns for A'a lava flow and pahochoc flow are resemble each other, while the curves for craters and lava flows are different from each other.

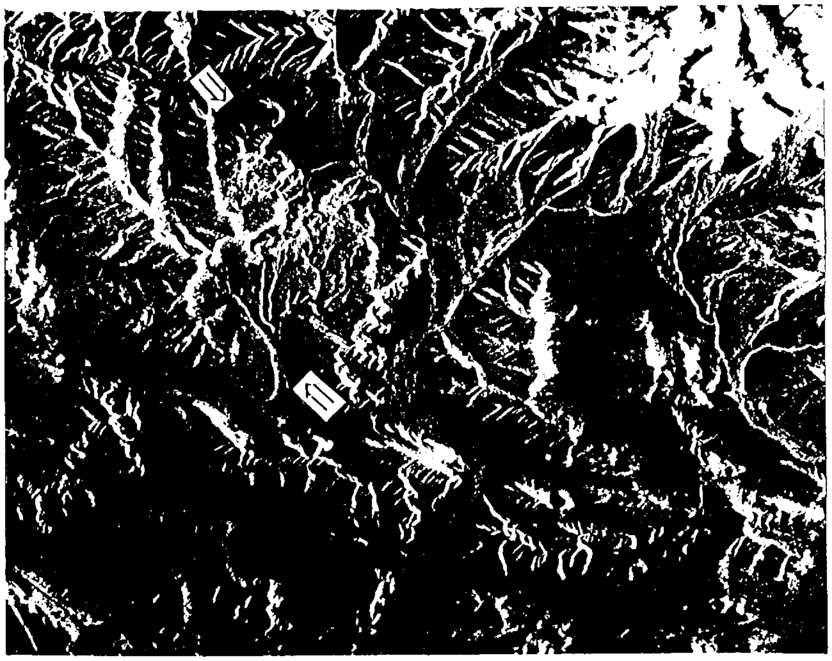

Fig. 7 ERS-1 SAR image with C-band VV polarization. The craters and pahoehoe lavas can be seen, but A'a lavas and calderas can not be distinguished from the image.

Table 1. SIR-C/X-SAR imaging Technical Parameters for the Study Area

Items	Imaging time	Plate Altitude	Wavelength (cm)	Polarization mode	Incidence angle	Swath width (km)	Resolution (m)	Pixel size (m)
Technical Parameters	17, Apr., 1994	215km	C (5.9) L (23.5)	HH, HV	47-53^{0}	50	30×30	12.5 ×12.5

Table 2. The response of different bands and different polarization radar to volcanic land forms

	Well preserved craters	Calderas	A'a lava	Pahoehoe lava	Escarpment
L-HH	√		+	$: _ . : -	+
L-HV	√	-1	√		√
C-HH	- i		+	+	+
C-HV	+	+	i	+	+
IRS- I SAR	-1		.	-1	"i

√ - dean be well discerned, + - Can be discerned, - -Can not be discerned